

Linear Quadratic Gaussian with noise signals for lateral and longitudinal of F-16

Nguyen Cong Danh^{1,*}

¹ The single author, District 2, HCMC, Vietnam

Abstract

Today, classical control methods are still widely used because of their excellent performance in a working environment with noise signals. Besides, they are suitable for functions of the system: operations to control a machine are more flexible, easy to perform, less unwanted risks occur, the efficiency of controlling a system better. In the early years of the 21st century, traditional algorithms still promote their effects. Besides the traditional control methods, the author has applied more modern and smarter algorithms such as adjusting Linear Quadratic Gaussian (LQG) to control a system on the ground or a system moving in the air. In the paper, LQG regulator is applied to a flight model to demonstrate its effectiveness in all cases. LQG regulator has not been applied before for this model. Results are as expected by the author for the working environment with noise signals affecting the system. Kalman filter used in this paper has shown its usefulness in the problem of dealing with unwanted signals. Simulation is done by Matlab.

Keywords: Linear Quadratic Gaussian (LQG), F-16, Kalman filter.

Received on 15 October 2022, accepted on 13 April 2023, published on 20 April 2023

Copyright © 2023 Nguyen Cong Danh *et al.*, licensed to EAI. This is an open access article distributed under the terms of the [CC BY-NC-SA 4.0](https://creativecommons.org/licenses/by-nc-sa/4.0/), which permits copying, redistributing, remixing, transformation, and building upon the material in any medium so long as the original work is properly cited.

doi: 10.4108/eetcasa.v9i1.2781

*Corresponding author. Email: congdanh.ptithcm@gmail.com

1. Introduction

The aviation industry is always an attractive topic for experts as well as many people. Humans have long observed flying objects at high altitudes. These objects are carefully analyzed for the characteristics of which they can fly. The development of science and technology has made the speed of flying objects change and they tend to fly faster and more agile [1]. The advent of drones aims to replace humans in its missions during emergencies or in harsh environments. Military autopilots require precise control of targets. Tests of autonomous flying devices were carried out very early on on a large scale [2]. Automatic in-flight control systems have been flexibly converted to suit the actual situation. Humans were then introduced into the cockpits of the planes, and the control systems [2] came into play in tasks such as navigation, and flight instrument display [3]. Aircraft have a six-degree-of-freedom motion, which is further split into translational (horizontal, vertical and

transverse) and rotational (pitch, roll and yaw) motions. Aircraft have three control surfaces (Rudder, Elevator and ailerons). This control surfaces supports the rotation of the aircraft. The lateral axis travel from wingtip-to-wingtip and the pitch motion is angular displacement about this axis. This allows the aircraft to fly higher or lower, depending on the angle that has been adjusted. Longitudinal axis passes through aircraft from nose-to-tail and motion about this axis is called roll motion. Pitch control can be achieved by providing change to elevator surface. Roll motion can be controlled with the help of ailerons while for yaw control the author needed to have a change in rudder surface [4]. Techniques to linearize a system and nonlinear approaches have been studied for implementation of survey plans [5-7]. So in a certain time and around the work point issues were well solved. Classical control methods have been applied to more complex structured systems. Systems in [8] are tested in the air at short ranges, before they are tested at longer ranges. The system of spacecraft launched into the air is the result of early tests [8]. Fuzzy controllers [9, 10] are used for generations of flying devices. UAV [11] is more and more

perfect with more modern functions thanks to its control methods. UAV has always been of interest to the author for artificial intelligence applications. Today, PID controller [12] is increasingly advanced to serve both civil and defense aviation systems. Besides, other control methods mentioned in [13, 14, 15] have been improved over the original method: Adaptive controller. Other techniques [16] for navigation, alarm sensors have also been refurbished so that the system can meet international quality standards. This is to bring satisfaction to customers during flights. Fuzzy controller [17] has been studied to develop into many next generations to serve many different purposes. Modern techniques [18] are gradually replacing old methods. However, disadvantages such as the handling of noise signals in [17,18] can not be completely resolved. This issue needs to be studied further by the author. Fuzzy controllers [19, 20] have been intensively studied theoretically and they have been implemented in practice, from the educational field [21] to the industrial field [22, 23]. In this paper, adjusting LQG is given in the context of a working environment where many undesirable effects have occurred, especially in the aviation environment, where it is difficult to have human intervention in the problem of noise signals. Therefore, this survey is extremely urgent. Previous articles have not addressed this issue.

2. System modeling linearization

The control of flight systems is derived from surveys on mathematical models. These mathematical models are established based on physical theories. The next section is the investigation of the stability of the flight system through control plans. These plans can change the original characteristics of the system and plans are programmed to control the operation of the system in accordance with stated expectations. Besides, other aspects must also be taken into account for their effect on the system such as the temperature inside the aircraft, the external environment can also affect the equipment. There are many ways for the author to approach the morphology of flying devices to meet the goals in the most effective way. The author has described the mathematical settings for a model that matches requirements of the problem [24]. Motions of an aircraft in a flight have been a focus of research to form equations that characterize this form [24]. These equations are based on fundamental laws of physics. According to Newton's law, equations of translational motion, equations of rotational motion are performed synchronously with each other [25].

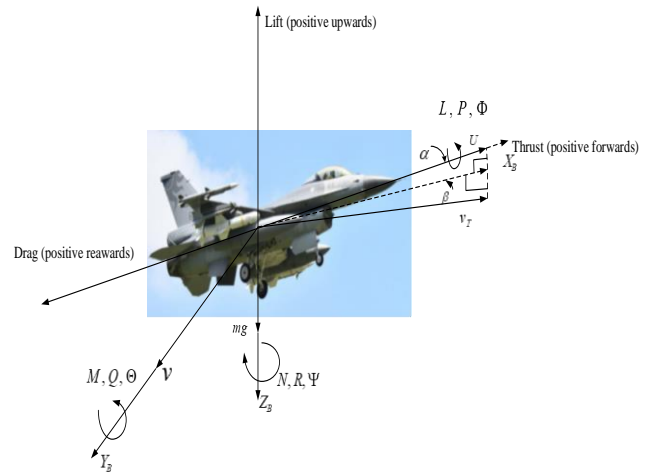


Figure 1. Moments, Euler angles and velocities of Aircraft.

Notes: U, V, R are forward, side and yaw velocity; L, M, N are roll, pitch and yaw moments; P, Q, R are angular velocities ; Φ, Θ, Ψ are roll, pitch and yaw angle. This is a type of F16 of any kind. This means that this model is a regular model. The author did not consider the military model or any other specific model. Therefore, this model does not have specific parameters for a particular type of fighter or military aircraft. There was no particular response of F-16 to the use of LQG regulator. This is the same for other systems. They are like that by default. For the translational dynamics:

$$\sum_B F = m\bar{a}_B \quad (1)$$

$$\bar{v}_B = \begin{bmatrix} U \\ V \\ W \end{bmatrix} \quad (2)$$

$$\bar{a}_B = \begin{bmatrix} \dot{U} \\ \dot{V} \\ \dot{W} \end{bmatrix} + \begin{bmatrix} P \\ Q \\ R \end{bmatrix} \times \begin{bmatrix} U \\ V \\ W \end{bmatrix} \quad (3)$$

$$\begin{bmatrix} U & V & W \end{bmatrix}^T$$

and

$$\begin{bmatrix} P & Q & R \end{bmatrix}^T$$

Represents translational and rotational velocities of flight.

$$\bar{F}_B = \begin{bmatrix} X \\ Y \\ Z \end{bmatrix} + L_{BV} \begin{bmatrix} 0 \\ 0 \\ mg \end{bmatrix} \quad (4)$$

Where $\begin{bmatrix} X & Y & Z \end{bmatrix}^T$ acting on Flight and $L_{BV} \begin{bmatrix} 0 & 0 & mg \end{bmatrix}^T$ represents weight vector .
Substituting Eq. (3) and (4) in Eq. (1) gives,

$$\begin{bmatrix} X \\ Y \\ Z \end{bmatrix} + L_{BV} \begin{bmatrix} 0 \\ 0 \\ mg \end{bmatrix} = m \left(\begin{bmatrix} \dot{U} \\ \dot{V} \\ \dot{W} \end{bmatrix} + \begin{bmatrix} P \\ Q \\ R \end{bmatrix} \times \begin{bmatrix} U \\ V \\ W \end{bmatrix} \right) \quad (5)$$

After simplifying Eq. (5) given translational dynamics can be achieved for a rigid body.

$$\begin{cases} X = m(\dot{U} - RV + QW + g \sin \theta) \\ Y = m(\dot{V} - WP + UR - g \cos \theta \sin \phi) \\ Z = m(\dot{W} - QU + VP - g \cos \theta \cos \phi) \end{cases} \quad (6)$$

For the rotatinal dynamics of aircraft.

The following moment equations represents the rotatinal form of Newton's second law.

$$\sum \vec{G}_B = \frac{d\vec{H}_B}{dt} \quad (7)$$

$$\vec{H}_B = I_B \vec{\omega}_B \quad (8)$$

\vec{H}_B is momentum of the system

$$\vec{\omega}_B = \begin{bmatrix} P \\ Q \\ R \end{bmatrix} \quad (9)$$

$$I_B = \begin{bmatrix} I_{XX} & I_{XY} & I_{XZ} \\ I_{XY} & I_{YY} & I_{YZ} \\ I_{XZ} & I_{YZ} & I_{ZZ} \end{bmatrix} \quad (10)$$

$\vec{\omega}_B$ and I_B are the angular velocity and Moment of inertia of the system respectively, substituting Eq. (7), (8) and (9) in Eq.(6) give us the Rotatinal dynamics of the system.

$$\begin{cases} L = I_x \dot{P} - I_{xz} (\dot{R} + PQ) + (I_z - I_y) QR \\ M = I_y \dot{Q} - I_{xz} (P^2 - R^2) + (I_x - I_y) PR \\ N = I_z \dot{R} - I_{xz} \dot{P} - (I_x - I_y) + I_{xz} RQ \end{cases} \quad (11)$$

The above derived translational and rotational equation were used along with disturbance forces and moments, gravitational terms, aerodynamics terms and power terms which are not mentioned here, to get the Longitudinal and lateral directional equations of motion.

3. State space representation of longitudinal and lateral equation

State space is achieved for both longitudinal and lateral motion as follows:

$$\begin{cases} \dot{x} = Ax + Bu \\ y = Cx + Du \end{cases} \quad (12)$$

The longitudinal dynamics from Eq. (12) are obtained in matrix form as

$$x = [\theta \quad v \quad \alpha \quad q]^T \quad u = [\delta_e] \quad y = [\theta \quad v \quad \alpha \quad q]^T$$

$$A = \begin{bmatrix} 0 & 0 & 0 & 1 \\ -32.1 & -0.013 & -2.66 & -1.18 \\ 0 & -0.0 & -0.67 & 0.93 \\ 0 & 0 & -0.57 & -0.87 \end{bmatrix} \quad B = \begin{bmatrix} 0 \\ 0.0387 \\ -0.0014 \\ -0.1188 \end{bmatrix}$$

$$C = \begin{bmatrix} 57.2958 & 0 & 0 & 0 \\ 0 & 1 & 0 & 0 \\ 0 & 0 & 57.2958 & 0 \\ 0 & 0 & 0 & 57.2958 \end{bmatrix} \quad D = \begin{bmatrix} 0 \\ 0 \\ 0 \\ 0 \end{bmatrix}$$

The transfer function of Longitudinal Dynamics

Model

$$G_1(s) = \frac{-6.807s + 4.606}{s^3 + 0.2s^2 - 0.0528s} \quad (13)$$

$$G_2(s) = \frac{0.0387s^3 + 0.1516s^2 + 4.014s - 2.581}{s^4 + 0.213s^3 - 0.0502s^2 - 0.0006864s} \quad (14)$$

$$G_3(s) = \frac{-0.08021s - 6.4}{s^2 + 0.2s - 0.0528} \quad (15)$$

$$G_4(s) = \frac{-6.807s + 4.606}{s^2 + 0.2s - 0.0528} \quad (16)$$

3.2. Lateral dynamics model

The lateral dynamics from Eq. (12) are obtained in matrix form as

$$x^T(t) = [\phi \quad \beta \quad p \quad r] \quad u^T(t) = [\xi \quad \zeta]$$

$$A = \begin{bmatrix} 0 & 0 & 1 & 0.078 \\ 0.064 & -0.202 & 0.078 & -0.99 \\ 0 & -22.92 & -2.25 & 0.54 \\ 0 & 6.0 & -0.04 & -0.31 \end{bmatrix}$$

$$B = \begin{bmatrix} 0 & 0 \\ 0.0002 & 0.0005 \\ -0.4623 & 0.0569 \\ -0.0244 & -0.0469 \end{bmatrix}$$

$$C = \begin{bmatrix} 57.29 & 0 & 0 & 0 \\ 0 & 57.29 & 0 & 0 \\ 0 & 0 & 57.29 & 0 \\ 0 & 0 & 0 & 57.29 \end{bmatrix}$$

3.1. Longitudinal dynamics model

$$D = \begin{bmatrix} 0 & 0 \\ 0 & 0 \\ 0 & 0 \\ 0 & 0 \end{bmatrix}$$

The transfer function of Lateral Dynamics Model

$$G_1(s) = \frac{3.05s^2 - 0.9491s - 42.13}{s^4 + 2.762s^3 + 8.964s^2 + 16.16s + 0.1754} \quad (17)$$

$$G_2(s) = \frac{0.02865s^3 + 2.988s^2 + 6.296s - 0.05902}{s^4 + 2.762s^3 + 8.964s^2 + 16.16s + 0.1754} \quad (18)$$

$$G_3(s) = \frac{3.26s^3 - 0.4385s^2 - 41.8s + 0.2098}{s^4 + 2.762s^3 + 8.964s^2 + 16.16s + 0.1754} \quad (19)$$

$$G_4(s) = \frac{-2.687s^3 - 6.547s^2 - 4.113s - 2.69}{s^4 + 2.762s^3 + 8.964s^2 + 16.16s + 0.1754} \quad (20)$$

4. Simulation results and discussions

Simulation results are shown Figures 2, 3, 4, 5, 6, 7, 8, 9, 10, 11, 12, 13, 14, 15, 16, 17, 18, 19, 20, 21, 22, 23, 24, 25, 26, 27, 28, 29, 30, 31, 32, 33, 34. Figures 3-34, describing their axes, the ultimate goal of the problem is to find the transfer function. A description of their axes is necessary to find the transfer function. The simulation results (Figures 3-34) 'reflect' the nature of LQG strategy in this model.

Model with using LQG regulator

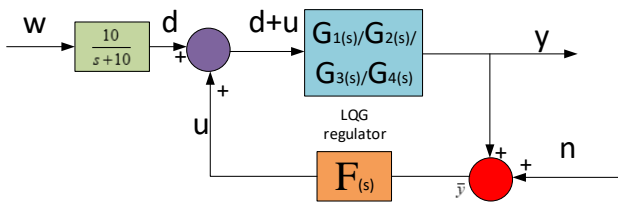


Figure 2. LQG regulator 'G(s)'

Figure 2: the value of 'd' is a color noise signal with a spectral density of less than 10 rad/s, the value of 'n' is a white noise signal $E(n^2) = 0.01$. The value of the quality

indicator 'J': $J(u) = \int_0^{\infty} (10y^2 + u^2) dt$. The model of the

$$\text{object: } \dot{x} = Ax + Bu + Bd, \bar{y} = Cx + n$$

Longitudinal Dynamics Model: The input data is the transfer function of Longitudinal Dynamics Model. They are $G_1(s)/G_2(s)/G_3(s)/G_4(s)$ in Figure 2. The output data is output signals of Longitudinal Dynamics Model and they are denoted by 'y' in Figure 2. These output signals are simulated in the Figures 3, 4, 5, 6, 7, 8, 9, 10, 11, 12, 13, 14, 15, 16, 17, 18.

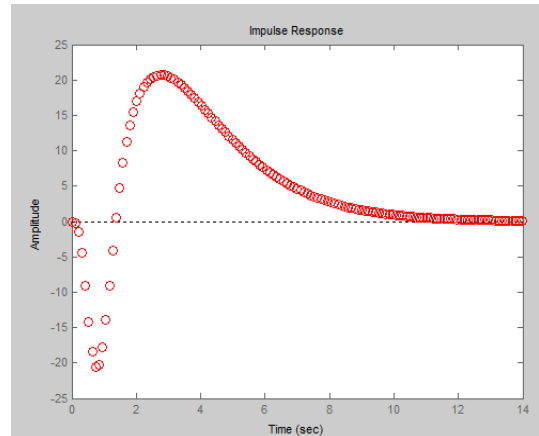


Figure 3. LQG regulator $G_1(s)$ for impulse response (The closed loop)

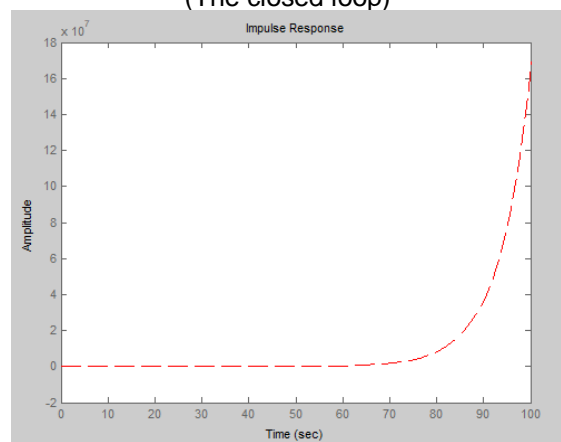


Figure 4. LQG regulator $G_1(s)$ for impulse response (The open loop)

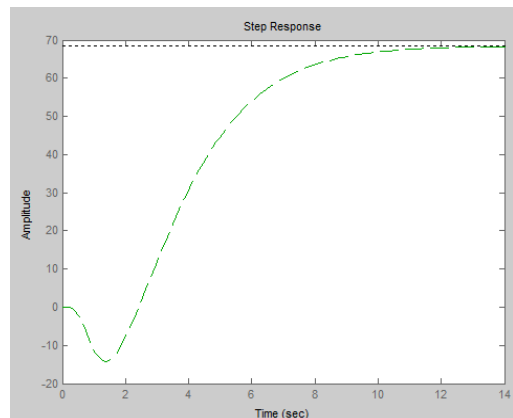


Figure 5. LQG regulator $G_1(s)$ for step response (The closed loop)

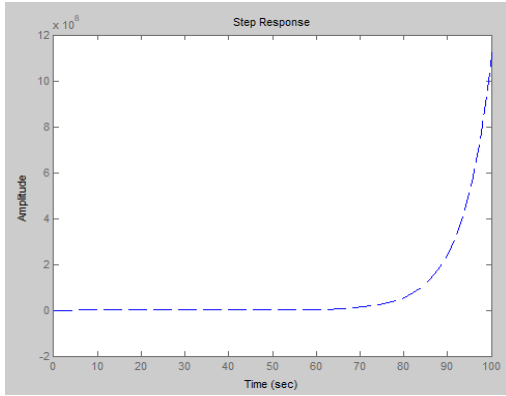


Figure 6. LQG regulator $G_1(s)$ for step response (The open loop)

Figure 3 shows that impulse response for the closed system (the signal is highlighted in red) is better than the open loop (the signal is highlighted in red in Figure 4). The value of the amplitude of the oscillation of the closed loop in this case is zero and the closed loop reaches a steady state. For LQG regulator, the closed loop responds well. The value of the amplitude of the oscillation of the open loop in this case is large and the open loop does not reach a steady state. Figure 5 shows that step response for the closed loop (the signal is highlighted in green) is better than the open loop (the signal is highlighted in blue in Figure 6). The value of the amplitude of the oscillation of the closed loop in this case is 70 and the closed loop reaches a steady state. For LQG regulator, the closed loop responds well. The value of the amplitude of the oscillation of the open loop in this case is large and the open loop does not reach a steady state. In general, LQG regulator, the system responds well to the presence of noise signals.

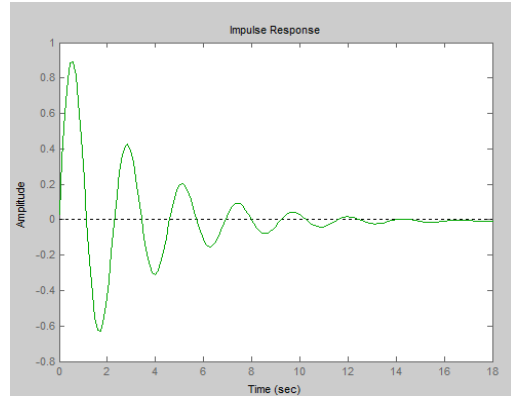


Figure 8. LQG regulator $G_2(s)$ for impulse response (The open loop)

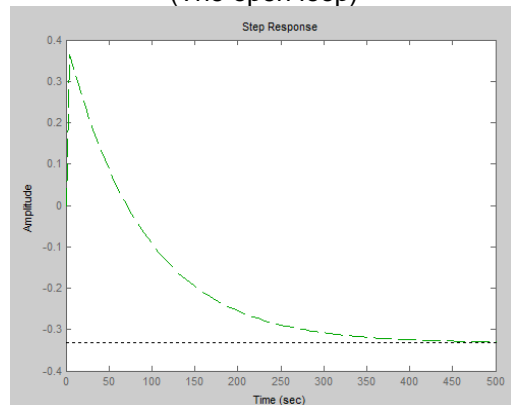


Figure 9. LQG regulator $G_2(s)$ for step response (The closed loop)

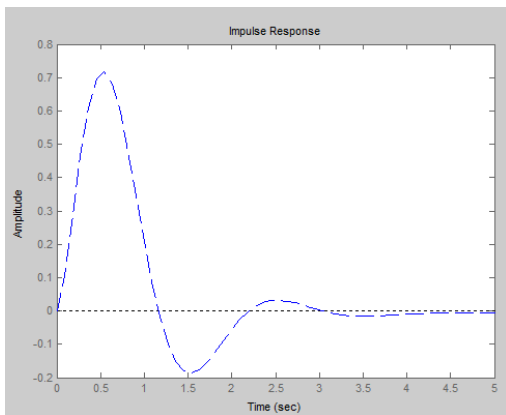


Figure 7. LQG regulator $G_2(s)$ for impulse response (The closed loop)

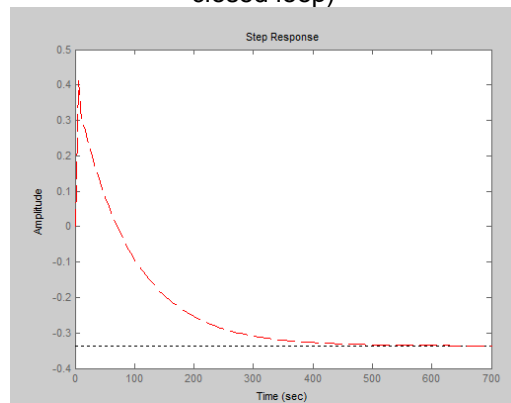


Figure 10. LQG regulator $G_2(s)$ for step response (The open loop)

Figure 7 shows that impulse response for the closed loop (the signal is highlighted in blue) is better than the open loop (the signal is highlighted in green in Figure 8). The value of the amplitude of the oscillation of the closed loop in this case is zero and the closed loop reaches a steady state. For LQG regulator, the closed loop and the open loop respond well. The value of the amplitude of the oscillation of the open loop in this case is 0.0 and the open loop reaches a steady state. Figure 9 shows that step response for the closed loop (the signal is highlighted in green) is better than the open loop (the signal is highlighted in red in Figure 10). The value of the amplitude of the oscillation of the closed loop in this case is -0.3 and the closed loop reaches a steady state. For LQG regulator, the closed loop responds well. The

value of the amplitude of the oscillation of the open loop in this case is -0.3 and the open loop reaches a steady state. In general, LQG regulator, the system responds well to the presence of noise signals.

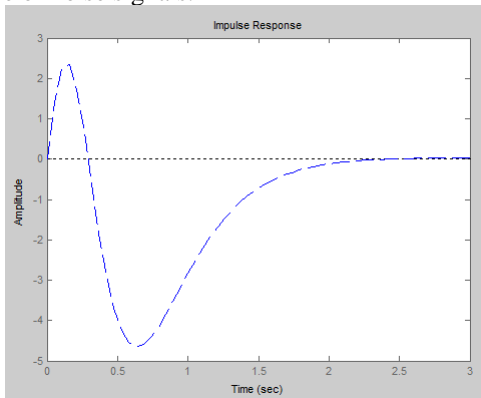


Figure 11. LQG regulator $G_3(s)$ for impulse response (The closed loop)

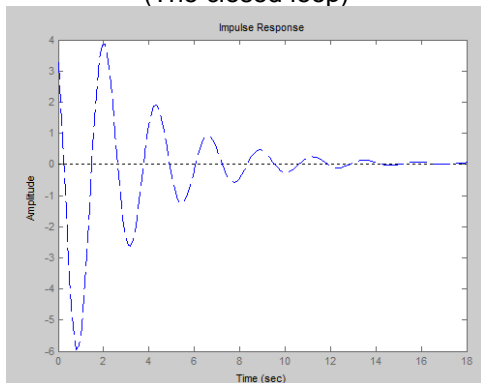


Figure 12. LQG regulator $G_3(s)$ for impulse response (The open loop)

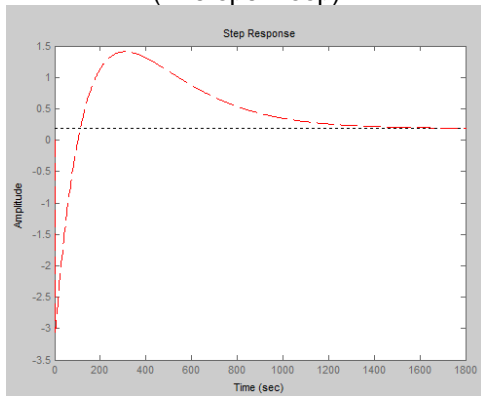


Figure 13. LQG regulator $G_3(s)$ for step response (The closed loop)

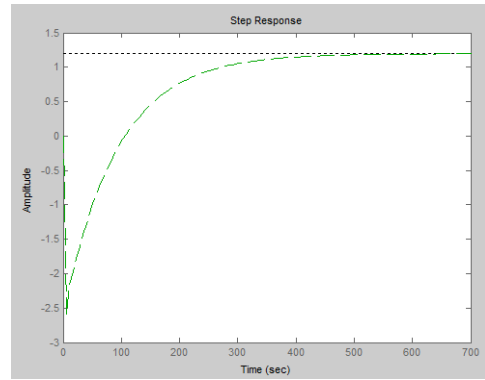


Figure 14. LQG regulator $G_3(s)$ for step response (The open loop)

Figure 11 shows that impulse response for the closed loop (the signal is highlighted in blue) is better than the open loop (the signal is highlighted in blue in Figure 12). The value of the amplitude of the oscillation of the closed loop in this case is zero and the closed loop reaches a steady state. For LQG regulator, the closed loop and the open loop respond well. The value of the amplitude of the oscillation of the open loop in this case is 0.0 and the open loop reaches a steady state. Figure 13 shows that step response for the closed loop (the signal is highlighted in red) is worse than the open loop (the signal is highlighted in green in Figure 14). The value of the amplitude of the oscillation of the closed loop in this case is zero and the closed loop reaches a steady state. For LQG regulator, the closed loop responds well. The value of the amplitude of the oscillation of the open loop in this case is 1.0 and the open loop reaches a steady state. In general, LQG regulator, the system responds well to the presence of noise signals.

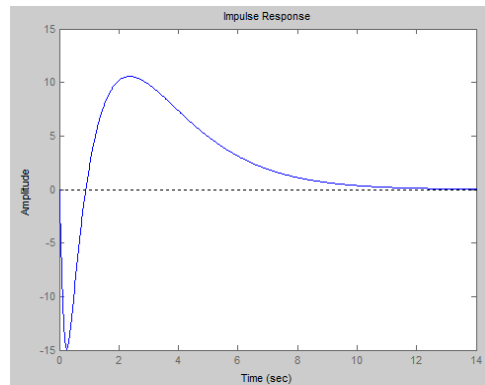


Figure 15. LQG regulator $G_4(s)$ for impulse response (The closed loop)

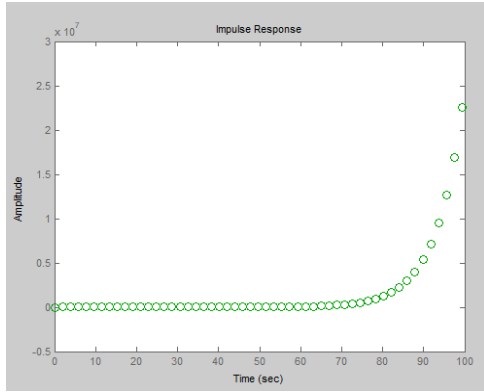


Figure 16. LQG regulator $G_4(s)$ for impulse response (The open loop)

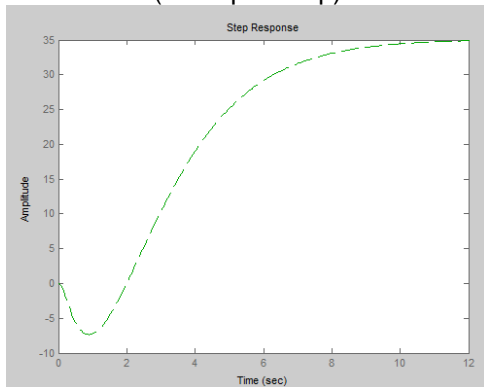


Figure 17. LQG regulator $G_4(s)$ for step response (The closed loop)

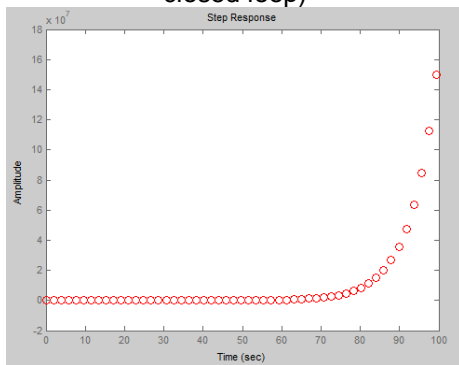


Figure 18. LQG regulator $G_4(s)$ for step response (The open loop)

Figure 15 shows that impulse response for the closed loop (the signal is highlighted in blue) is better than the open loop (the signal is highlighted in green in Figure 16). The value of the amplitude of the oscillation of the closed loop in this case is zero and the closed loop reaches a steady state. For LQG regulator, the closed loop responds well. The value of the amplitude of the oscillation of the open loop in this case is large and the open loop does not reach a steady state. Figure 17 shows that step response for the closed loop (the signal is highlighted in green) is better than the open loop (the signal is highlighted in red in Figure 18). The value of the amplitude of the oscillation of the closed loop in this case is 35 and the closed loop reaches a steady state. For LQG regulator, the closed loop responds well. The value of the amplitude of the oscillation of the open loop in this case is large and the open loop does not

reach a steady state. In general, LQG regulator, the system responds well to the presence of noise signals.

Lateral Dynamics Model: The input data is the transfer function of Lateral Dynamics Model. They are $G_1(s)/G_2(s)/G_3(s)/G_4(s)$ in Figure 2. The output data is output signals of Longitudinal Dynamics Model and they are denoted by 'y' in Figure 2. These output signals are simulated in the Figures 19, 20, 21, 22, 23, 24, 25, 26, 27, 28, 29, 30, 31, 32, 33, 34.

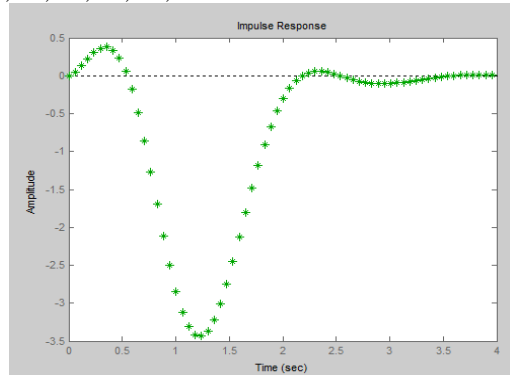


Figure 19. LQG regulator $G_1(s)$ for impulse response (The closed loop)

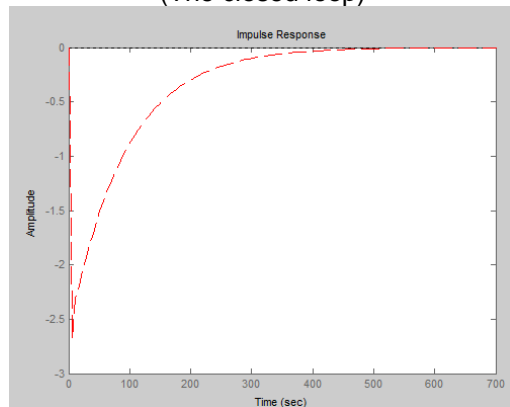


Figure 20. LQG regulator $G_1(s)$ for impulse response (The open loop)

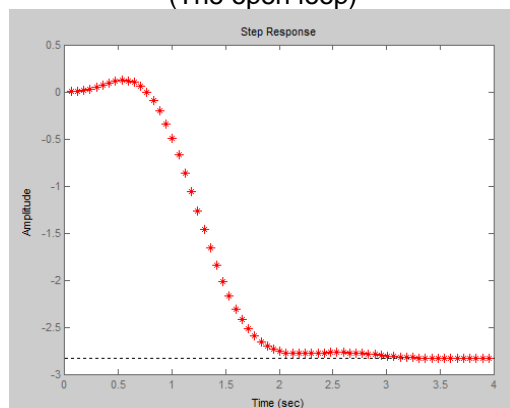


Figure 21. LQG regulator $G_1(s)$ for step response (The closed loop)

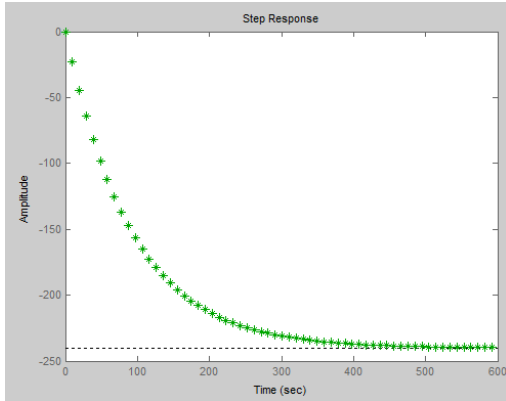


Figure 22. LQG regulator $G_1(s)$ for step response (The open loop)

Figure 19 shows that impulse response for the closed loop (the signal is highlighted in green) is better than the open loop (the signal is highlighted in red in Figure 20). The value of the amplitude of the oscillation of the closed loop in this case is zero and the closed loop reaches a steady state. For LQG regulator, the closed loop and the open loop respond well. The value of the amplitude of the oscillation of the open loop in this case is 0.0 and the open loop reaches a steady state. Figure 21 shows that step response for the closed loop (the signal is highlighted in red) is better than the open loop (the signal is highlighted in green in Figure 22). The value of the amplitude of the oscillation of the closed loop in this case is -3 and the closed loop reaches a steady state. For LQG regulator, the closed loop responds well. The value of the amplitude of the oscillation of the open loop in this case is -250 and the open loop reaches a steady state. In general, LQG regulator, the system responds well to the presence of noise signals.

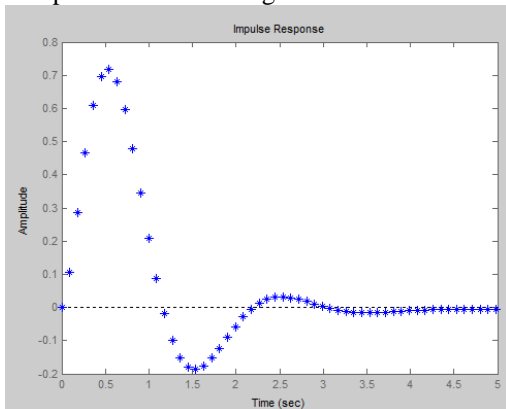


Figure 23. LQG regulator $G_2(s)$ for impulse response (The closed loop)

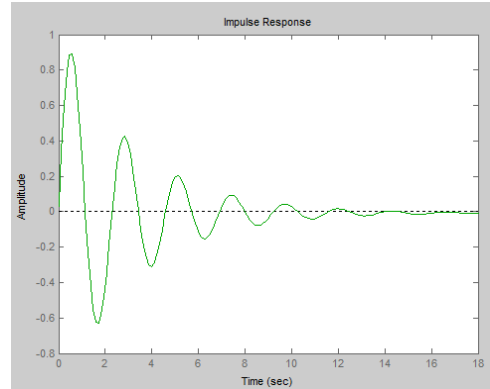


Figure 24. LQG regulator $G_2(s)$ for impulse response (The open loop)

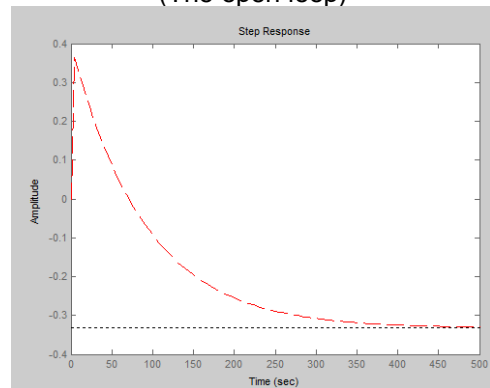


Figure 25. LQG regulator $G_2(s)$ for step response (The closed loop)

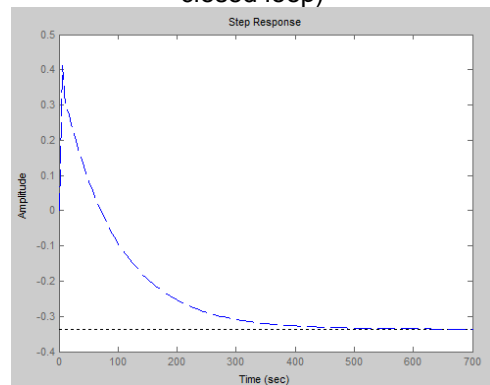


Figure 26. LQG regulator $G_2(s)$ for step response (The open loop)

Figure 23 shows that impulse response for the closed loop (the signal is highlighted in blue) is better than the open loop (the signal is highlighted in green in Figure 24). The value of the amplitude of the oscillation of the closed loop in this case is zero and the closed loop reaches a steady state. For LQG regulator, the closed loop and the open loop respond well. The value of the amplitude of the oscillation of the open loop in this case is 0.0 and the open loop reaches a steady state. Figure 25 shows that step response for the closed loop (the signal is highlighted in red) is better than the open loop (the signal is highlighted in blue in Figure 26). The value of the amplitude of the oscillation of the closed loop in this case is -0.3 and the closed loop reaches a steady state. For LQG regulator, the closed loop responds well. The value of the amplitude of the oscillation

of the open system in this case is -0.3 and the open loop reaches a steady state. In general, LQG regulator, the system responds well to the presence of noise signals.

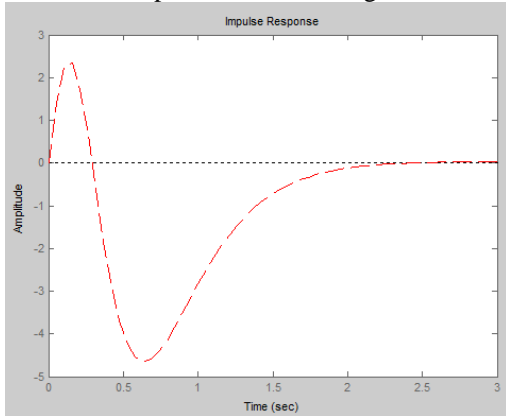


Figure 27. LQG regulator $G_3(s)$ for impulse response (The closed loop)

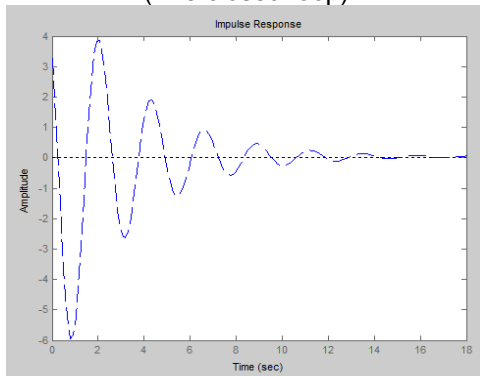


Figure 28. LQG regulator $G_3(s)$ for impulse response (The open loop)

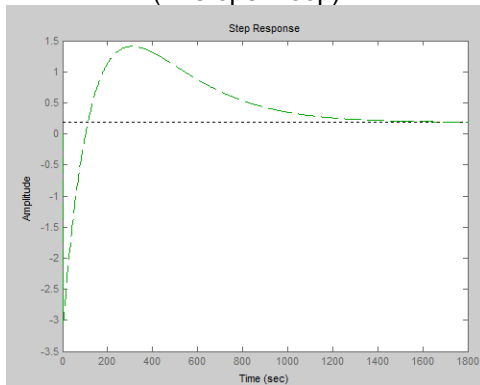


Figure 29. LQG regulator $G_3(s)$ for step response (The closed loop)

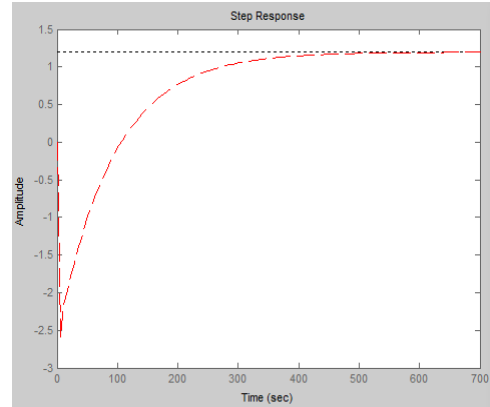


Figure 30. LQG regulator $G_3(s)$ for step response (The open loop)

Figure 27 shows that impulse response for the closed loop (the signal is highlighted in red) is better than the open loop (the signal is highlighted in blue in Figure 28). The value of the amplitude of the oscillation of the closed loop in this case is zero and the closed loop reaches a steady state. For LQG regulator, the closed loop and the open loop respond well. The value of the amplitude of the oscillation of the open loop in this case is 0.0 and the open loop reaches a steady state. Figure 29 shows that step response for the closed loop (the signal is highlighted in green) is worse than the open loop (the signal is highlighted in red in Figure 30). The value of the amplitude of the oscillation of the closed loop in this case is zero and the closed loop reaches a steady state. For LQG regulator, the closed loop responds well. The value of the amplitude of the oscillation of the open system in this case is 1.0 and the open loop reaches a steady state. In general, LQG regulator, the system responds well to the presence of noise signals.

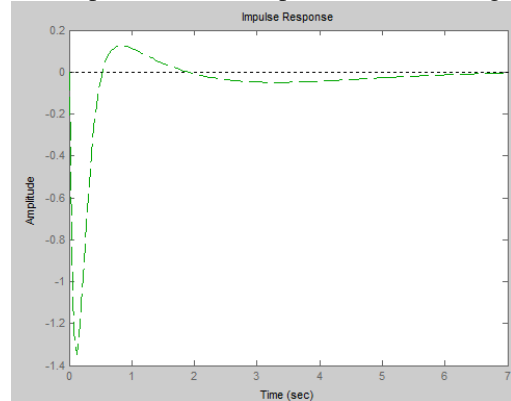


Figure 31. LQG regulator $G_4(s)$ for impulse response (The closed loop)

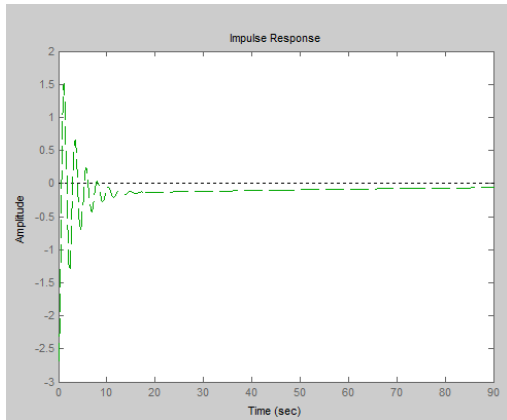


Figure 32. LQG regulator $G_4(s)$ for impulse response (The open loop)

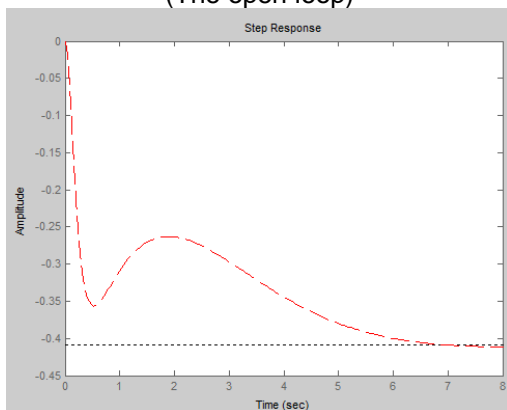


Figure 33. LQG regulator $G_4(s)$ for step response (The closed loop)

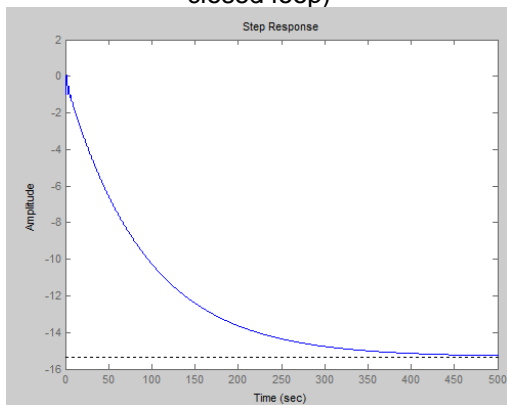


Figure 34. LQG regulator $G_4(s)$ for step response (The open loop)

Figure 31 shows that impulse response for the closed loop (the signal is highlighted in green) is better than the open loop (the signal is highlighted in green in Figure 32). The value of the amplitude of the oscillation of the closed loop in this case is zero and the closed loop reaches a steady state. For LQG regulator, the closed loop and the open loop respond well. The value of the amplitude of the oscillation of the open loop in this case is 0.0 and the open loop reaches a steady state. Figure 33 shows that step response for the closed loop (the signal is highlighted in red) is better than the open loop (the signal is highlighted in blue in Figure 34). The value of the amplitude of the oscillation of the closed loop in this case is -0.4 and the closed loop

reaches a steady state. For LQG regulator, the closed loop responds well. The value of the amplitude of the oscillation of the open loop in this case is -16 and the open loop reaches a steady state. In general, LQG regulator, the system responds well to the presence of noise signals.

5. Conclusions

Through this survey, it is more efficient to use LQG regulator for Lateral Dynamics Model than Longitudinal Dynamics Model. Simulation results show that the steady state achieved by Lateral Dynamics Model is much better than that of Longitudinal Dynamics Model. Overall, the effect of this method is excellent and it is ideal for flying models. In the future, modern control methods can be applied to manned aircraft as well as unmanned aerial vehicles to confirm the role of methods in civil aviation.

References

- [1] Stevens, B. L., Lewis, F. L., & Johnson, E. N. (2015). Aircraft control and simulation: dynamics, control design, and autonomous system. John Wiley & Sons.
- [2] Ji Hong Zhu. A survey of Advanced Flight control theory and Application. IMACS Multi conference on Computational Engineering in System Application (CESA). 2006, 1: 655-658.
- [3] Z Peng, L Jikai. On new UAV flight control system based on Kalman & PID. IEEE Transaction, International Conference on Harbin. 2011, 2: 819-823.
- [4] McRuer, Duane T., Dunstan Graham, and Irving Ashkenas. Aircraft dynamics and automatic control. Vol. 740. Princeton University Press, 2014.
- [5] Ohri, J. (2014, December). GA turned LQR and PID controller for aircraft pitch control. In 2014 IEEE 6th India International Conference on Power Electronics (IICPE) (pp. 1-6). IEEE.
- [6] Usta, M. A., Akyazi, Ö., & Akpınar, A.S. (2011, June). Aircraft roll control system using LQR and fuzzy logic controller. In 2011 International Symposium on Innovations in Intelligent Systems and Applications (pp. 223-227), IEEE.
- [7] Hajiyevev, C., & Vural, S. Y. (2013). LQR controller with Kalman estimator applied to UAV longitudinal dynamics. Positioning, 4 (1), 36.
- [8] MR Rahimi, R Ghasemi, D Sanaei. Designing Discrete Time Optimal Controller for Double inverted pendulum system. International Journal on Numerical and Analytical Methods in Engineering. 2013; 1(1): 3-7.
- [9] W Dwiono. Fuzzy PI Controllers Performance on Boost Converter. International Journal of Electrical and Computer Engineering. 2013; 3(2): 215-220.
- [10] MRI Sheikh, T Junji. Smoothing Control of Wind Farm Output Fluctuations by Fuzzy Logic Controlled SMES. International Journal of Electrical and Computer Engineering. 2011; 1(2): 119-134.
- [11] Z Peng, L Jikai. On new UAV flight control system based on Kalman & PID. IEEE Transaction, International Conference on Harbin. 2011; 2: 819-823.
- [12] X Zhou, Z Wang, H Wang. Design of Series Leading Correction PID Controller. IEEE Conference. 2009.
- [13] L Yu, D Dipankar, T Gang. Modeling and multivariable adaptive control of aircraft with synthetic jet actuators. IEEE

- International Conference on Congress on Intelligent Control and Automation. 2008: 2192-2199.
- [14] Nambisant PR, Singh SN. Adaptive variable structure control of aircraft with an unknown high-frequency gain matrix. *Journal of Guidance, Control, and Dynamics*. 2008; 31(1): 194-203.
- [15] Young A. Adaptive control design methodology for nonlinear-in-control systems in aircraft applications. *Journal of Guidance Control and Dynamics*. 2007; 30(6): 1770-1782.
- [16] Ji-Hong Zhu. A Survey of Advanced Flight Control Theory and Application. IMACS Multi conference on Computational Engineering in System Application (CESA). 2006; 1: 655-658.
- [17] Kazemian HB. Developments of fuzzy PID controllers. *Expert Systems*. Nov2005; 22(5): 254-264.
- [18] H Ogata. *Modern Control Engineering*. New Jersey: Prentice Hall International Inc. 1997.
- [19] CC Lee. Fuzzy Logic in Control System: Fuzzy Logic Controller I. *System, Man and Cybernatics, IEEE Transaction*. 1990; 20: 404-418.
- [20] C C Lee. Fuzzy Logic in Control System: Fuzzy Logic Controller II. *System, Man and Cybernatics, IEEE Transaction*. 1990; 20: 419-435.
- [21] EH Mamdani. Application of fuzzy logic to approximate reasoning using linguistic synthesis. *IEEE Trans, Computer*. 1977; C-26(12): 1182-1191.
- [22] PJ King, EH Mamdani. The application of fuzzy control systems to industrial processes. *Automat*. 1977; 13(3): 235-242.
- [23] E H Mamdani. Application of fuzzy algorithms for simple dynamic plant. *Proc IEE*. 1974; 121(12):1585-1588.
- [24] Noth, A., Bouabdallah, S., & Siegwart, R. (2006). Dynamic modeling of fixed-wing uavs. *Autonomous System Laboratory Report, ETH, Zurich*.R.
- [25] C. Nelson, 1998, *Flight Stability and Automatic Control*, McGraw Hill, Second Edition.